

# Comparison and correlation of computer simulations using the finite element method and the SimSolid software with meshfree method for automotive durability analyses

Jefferson S. Carvalho<sup>1</sup>, Samir S. Saliba<sup>1</sup>, Robinson F. Barbosa<sup>2</sup>, Andre L.U. Penna<sup>2</sup>, Gabriel F. R. P. Justo<sup>2</sup>

<sup>1</sup>*Fiat Chrysler Automobiles*

*Avenida Contorno, 3455, 32669-900, Betim/MG, Brazil*

*jefferson.carvalho@fcagroup.com, samir.saliba@fcagroup.com*

<sup>2</sup>*Altair Engineering do Brasil*

*Rua Sampaio Viana, 277, 04004-000, São Paulo/SP, Brazil*

*robinson@altair.com, andrepenna@altair.com, gabrieljusto@altair.com*

**Abstract.** This paper presents an investigation comparing the finite element method to a meshfree method in the simulation of structural tests of different nature used in the automotive industry. In this study, the commercial softwares Altair OptiStruct and Altair SimSolid have been used, in order to know the ability of each one to reproduce the behaviour of the structure according to the imposed loading. For this, the numerical results were compared to experimental tests and briefly discussed.

**Keywords:** FEM, Meshfree, OptiStruct, SimSolid, Durability.

## 1 Introduction

The use of tools for virtual analyses today is vital in the development of automotive projects, whether applied to comfort, manufacturing or performance. For this last requirement specifically, the finite element method (FEM) is the tool that stands out the most as mentioned by Liu and Quek [1], being applied in all areas that design a vehicle, such as Noise, Vibration and Harshness (NVH), Safety and Durability. For the use of FEM is necessary to create meshes that describes the domain to be analyzed and this task in many cases takes up a considerable amount of work as well as it requires qualified professionals to perform this role with authority, once the result obtained is partially a consequence of the mesh quality, Wang, Botkin, Wu and He [2].

To overcome some drawbacks that come from the mesh, the use of the meshfree methods (MM) has been growing in the context of automotive industry, as presented in a work of Wang, Wu, Guo and Botkin [3], with its performance in the post-processing of the analyses, something of common interest among simulation engineers once the benefits of pre-processing have been seen. In view of that, this paper aims to compare and correlate the results achieved by both numerical methods with the ones from the experimental tests, for a linear, nonlinear and a modal analysis, all these referring to the perimeter of durability for passenger vehicles.

## 2 Numerical methods

The solution procedure of finite element and meshfree methods is rather similar as presented by Liu and Gu [4] but it mainly differs from each other due to the process in obtaining the shape functions. In FEM, the shape functions are constructed based on predefined elements from a generated mesh, while in MM, they are formulated from the nodes of the support domain as shown on the flowchart of Fig. 1 and outlined on the next subsections.

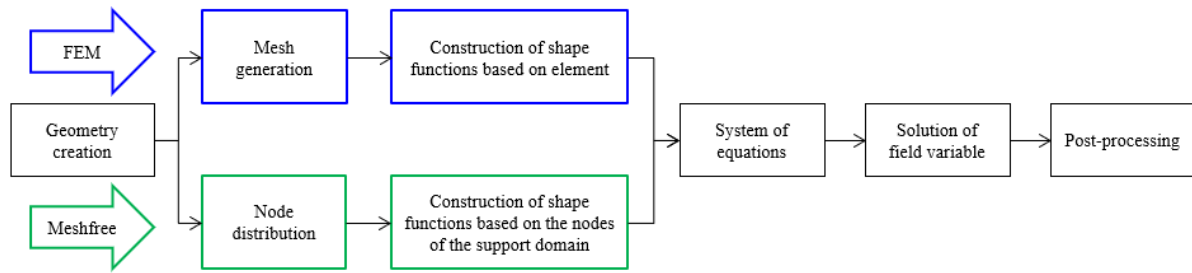


Figure 1. Flowcharts for FEM and MM

## 2.1 Finite element method

According to Oñate [5], in FEM is necessary to create a mesh on the geometry of the problem to be analyzed. This step is done by discretizing this domain into elements that are connected together with specific and predefined shapes such as quadrilaterals and triangles. There are shape functions for each type of form, which interpolate the nodal values and thus, the displacement field of the element can be known.

Concerning to this work FEM simulations, the commercial code OptiStruct was chosen using elements in two dimensions with basis on Reissner-Mindling shell theory, having three and four nodes, known as CTRIA3 and CQUAD4, respectively, and in three dimensions with six and eight nodes, CPENTA and CHEXA, in this order. This information can be found in Altair [6].

The elements cited above are with  $C^0$  continuity, therefore, as cited in Oñate [5], their shape functions can be obtained by the product of Lagrange polynomials. Regarding the two-dimensional elements, these expressions are writing in area coordinates  $L_1, L_2$  e  $L_3$  for the triangular element, and in the natural coordinate system  $\zeta, \eta$  for the quadrilateral one. In this way, represented by  $N$  and defined for each element node  $i$ , these shape functions are expressed in ZienKiewicz, Taylor and Zhu [7] and given in eq. (1) and eq. (2) for the CTRIA3 and CQUAD4 elements, respectively.

$$N_i = L_i ; i=1, 2, 3. \quad (1)$$

$$N_i = \frac{1}{4} (1 + \zeta \zeta_i) (1 + \eta \eta_i) ; i=1, 2, 3, 4. \quad (2)$$

The solid elements follow analogously to the shell ones. Volumetric coordinates  $L_1, L_2, \dots, L_6$  and natural system  $\zeta$  for CPENTA element, shape functions according to eq. (3)

$$N_i = \frac{1}{2} L_i (1 + \zeta \zeta_i) ; i=1, 2, \dots, 6. \quad (3)$$

For CHEXA element, natural coordinates  $\zeta, \eta, \zeta$ , equations expressed by eq. (4)

$$N_i = \frac{1}{8} (1 + \zeta \zeta_i) (1 + \eta \eta_i) (1 + \zeta \zeta_i) ; i=1, 2, \dots, 8. \quad (4)$$

The full integration technique was adopted to compute the stiffness matrix of the involved elements, since reduced integration can induce spurious zero-energy modes additionally to the natural zero-energy modes or the rigid body modes, as highlighted in Soriano [8].

## 2.2 Meshfree method

Consonant with Liu and Gu [4], a meshfree method is the one that is able to establish system equations for the whole domain without using a mesh to discretize it. Hence, in general, in meshfree methods the domain is discretized by a set of nodes distributed, randomly or regularly, and free of any type of relationship. Based on this nodal distribution which density is normally related to the accuracy required, support domains are defined from interest points and these domains represent a set of nodes that are used in the shape functions construction.

There are many methods which can be applied in the construction of shape functions. According to Liu [9], these methods fall into the following categories: integral representation methods (Smoothed particle hydrodynamics method, Reproducing kernel particle method, General reproducing method), series representation methods (Moving least square methods, Point interpolation methods, Partition of unit methods, Least squares methods, Finite element methods), differential representation methods (Finite difference method, Finite point method) and gradient smoothing methods.

It is normally used for the meshfree formulation the strong-form, weak-form or weakened-weak. Each one of them combined with the chosen method for shape function construction, gives to the meshfree method interesting and unique aspects.

The simulations of this paper applying the meshfree method were performed in the commercial software SimSolid [10], which type of method is not available for the users.

It is capable to run structural, dynamic and thermal analyses. To use meshfree method in this program, the model to be analyzed even in three-dimensions does not need to have simplifications, being thus closer to the real problem. In order to improve the accuracy, the shape function is defined in respect of the kind of problem besides the nodal distribution which is done using an adaptive algorithm that can enrich locally or globally the problem domain. This software can also automatically recognize the connections (e.g., welds, bolts) and the existing contacts on assemblies.

### 3 Simulations

In this section, three typical automotive durability analyses are presented comparing the results performed with the numerical methods related previously with the experimental data obtained from the bench tests. These simulations employ a problem of a linear and a nonlinear static nature and also a dynamic case applying a modal analysis.

These samples are all composed of steel materials with their sheet metals connected by spot welds, adhesives and bolts. The boundary conditions are shown with the fixed degrees of freedom (D.O.F), being 1, 2 and 3 the translations in the X, Y and Z directions, respectively, and 4, 5 and 6 the rotations in the same directions with all components of motion referred to the global axis of the figures. The applied load  $F$  is also shown in the static cases.

#### 3.1 Linear static analysis

Figure 2 displays a car body rear compartment of a pickup vehicle, which has some holes to fix the cargo retaining hooks. A stiffness analysis was performed in two hook anchorage points, position 1 and 2, and using the boundary conditions as Fig. 3 illustrates. The sheet metal components were characterized by a Young's modulus  $E = 205000$  MPa and a Poisson's ratio  $\nu = 0.3$ .

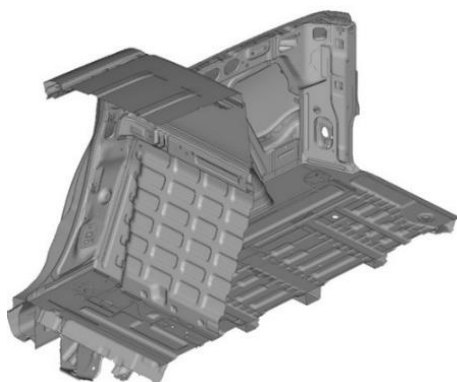


Figure 2. Car body of a pickup vehicle

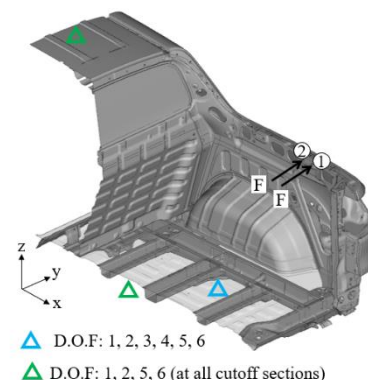


Figure 3. Car body boundary conditions

The results of this test are presented in Tab. 1 with the stiffness of each point denoted as the symbol  $k$ , and the percentage error from the numerical methods to the experimental test.

Table 1. Results of the stiffness analysis

Point	Experimental	OptiStruct		SimSolid	
	$k$ [N/mm]	$k$ [N/mm]	% error	$k$ [N/mm]	% error
1	375.5	351.3	-6.4	393.7	+4.8
2	379.8	363.2	-4.4	387.1	+1.9

Results agree well with those obtained with OptiStruct, an error less than -6.5 %. It ensures that the standard FEM approach is robust and the mesh size of 7 mm used in this sample is suitable for this type of analysis.

A similar error was found using SimSolid, maximum of +4.8 % in the measurement points. This is also an adequate performance for a stiffness simulation.

The two models showed thus, a good performance for this car body hook anchorage points, and the FEM case presented a more conservative result.

Regarding the models of the numerical methods, the total number of D.O.F in FEM were 1361878 while in MM were 2739762, a difference of 101.2 % due to the strategy of a high-level adaptive refinement in MM applied in 19.1 % of the model and done in 4 passes.

### 3.2 Nonlinear static analysis

Figure 4 shows an opened hood which is supported by a rod. To know the resistance of this rod, a force  $F$  was applied to the hood striker until the collapsing of the rod. The boundary conditions applied in this analysis are shown in Fig. 5 and the material properties in Tab. 2.



Figure 4. Hood

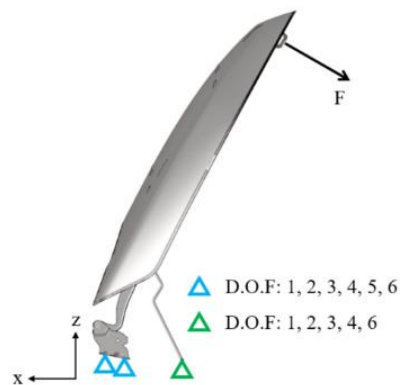


Figure 5. Hood boundary conditions

Table 2. Hood material properties

Component	Young's modulus [MPa]	Poisson's ratio	Yield stress [MPa]	Ultimate stress [MPa]
Outer panel	205000	0.3	258	401
Inner panel	205000	0.3	195	404
Hinges	205000	0.3	422	558
Reinforcements	205000	0.3	357	550
Strike	205000	0.3	449	650
Prop rod	205000	0.3	321	423

The force-displacement curve of the simulation is plotted according to Fig. 6, where the X axis represents the displacement measured on the top of the rod and the Y axis indicates the load on the hood striker.

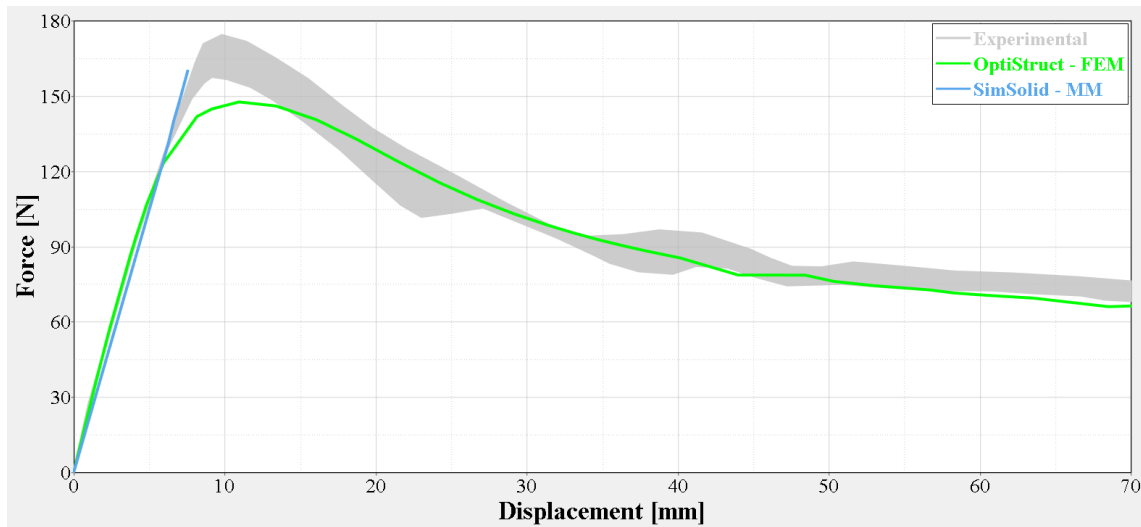


Figure 6. Nonlinear results

As it can be observed from the graphic, SimSolid matches well using loads up to 160 N although the implementation presented in the current version of the software (version 2020) works only for problems with small strain, i.e. 4.0 % of plastic strain. The problem had a plastic strain around 10.0 %, thus it was not possible to analyze the comparison between the numerical results. On the other hand, the OptiStruct model presented a behaviour very close to that obtained in the experimental test. The FEM model was able to adequately reproduce the linear state of the structure as it can be seen in the linear branch and represented the softening branch satisfactorily. The maximum load was 6.5 % below that found in the experimental test, which is a small error.

In relation to the models of the numerical methods for this sample, the total number of D.O.F in FEM were 448795 while in MM were 5021407, a difference of 1018.9 % due to the strategy of a high-level adaptive refinement in MM applied in 82.4 % of the model and done in 5 passes.

### 3.3 Natural frequency analysis

The decklid that is given in Fig. 7, was subjected to a natural frequency analysis in order to know its first mode. For this purpose, the Lanczos method was used in the numerical simulation. The applied boundary conditions are represented in Fig. 8 and the sheet metal components were characterized by a Young’s modulus  $E = 205000$  MPa and a Poisson’s ratio  $\nu = 0.3$ .



Figure 7. Decklid

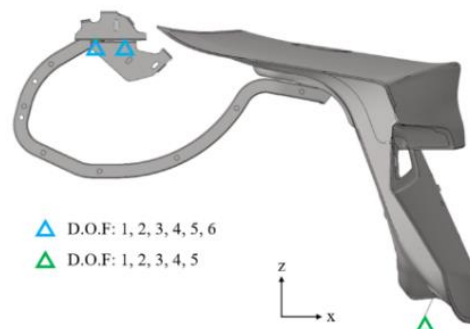


Figure 8. Decklid boundary conditions

The experimental test was done using nine measurement points positioned in the decklid surface as Fig.9 illustrates by *PM\_01*, *PM\_02*, ..., *PM\_09*. The force was inserted in the structure in the *PM\_04* and *PM\_06* locations by a modal hammer. The decklid presented its first mode with a frequency of 16.3 Hz and a mode shape of torsion related to the global X axis as shown in Fig.9.

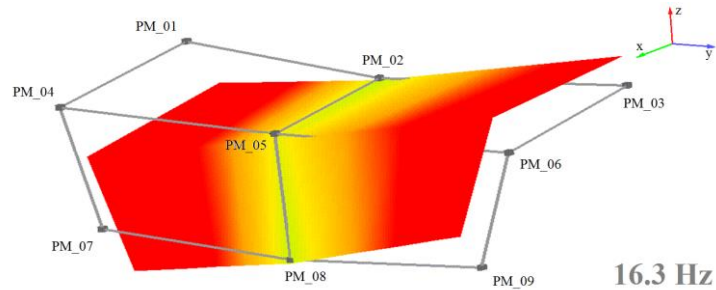


Figure 9. Decklid experimental modal analysis

The results of the virtual analyses are shown in Fig. 10 and Fig. 11 for OptiStruct and SimSolid programs, respectively, and in Tab. 3 together with the experimental data. These images are in a scale factor of 5.

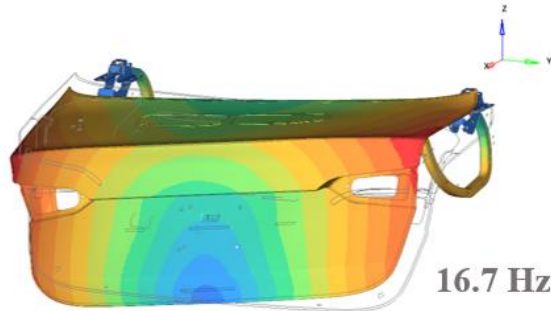


Figure 10. Decklid OptiStruct modal analysis

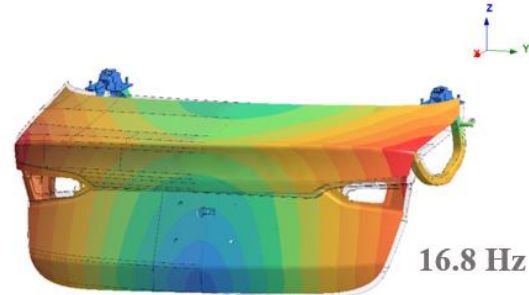


Figure 11. Decklid SimSolid modal analysis

Table 3. Results of the modal analysis

Mode	Experimental	OptiStruct		SimSolid	
	[Hz]	[Hz]	% error	[Hz]	% error
First	16.3	16.7	+2.5	16.8	+3.1

The OptiStruct modal frequency of 16.7 Hz represents a highly accurate value with an error of +2.5 % and also, the mode shape around the X axis fitted exactly the experimental one.

SimSolid equivalently performed the same mode and a frequency of 16.8 Hz, which means also in a very small percentage error of +3.1 %. Since the two results had the same mass value and distribution, the meshfree one is slightly stiffer probably due its hem modeling, i.e., the wrapping process of the decklid outer panel flange around the inner panel flange that was modeled with a rigid connection between the flanges into the whole perimeter of interface, while in FEM with merged nodes.

It was noticed, therefore, that both virtual tests led to a satisfactory performance of frequency magnitude as well as the mode shape which reproduced correctly the physical behaviour.

Concerning to the models of the numerical methods in this frequency analysis, the total number of D.O.F in FEM were 581077 while in MM were 8288048, a difference of 1326.3 % due to the strategy of a standard level adaptive refinement in MM applied in 100.0 % of the model and done in 5 passes.

## 4 Conclusion

A brief investigation, carried out with three numerical simulations, compared the results obtained by the finite element method, using the Altair OptiStruct software, and a meshfree method, using the Altair SimSolid software, with the results obtained in experimental tests.

In linear static analysis, according to Tab. 1, the results of both softwares/methods are considered satisfactory, since the difference in comparison to the experimental test was within the acceptable range. In the nonlinear analysis, the FEM model reproduced the force-displacement curve of the experimental test almost completely (Fig. 6), only the maximum load was 6.5 % lower. Finally, in the natural frequency analysis, the numerical models were able to reproduce the first mode of the experimental test and also very accurate frequency values were found, as it can be seen in Tab. 3.

In general, the models analyzed with both softwares reproduced the tests well, presenting results similar to those obtained experimentally.

In particular, for the authors all models were able to provide satisfactory results within their possibilities. Although it was not the aim of the paper, the time saved in building the models in SimSolid is significant, however it is necessary that the simulation engineers have experience to model certain connections in order to avoid influences on the results.

**Acknowledgements.** The authors would like to acknowledge *Fiat Chrysler Automobiles* Department of Virtual and Experimental Analyses and *Altair Engineering do Brasil* to their support for this work.

**Authorship statement.** The authors hereby confirm that they are the sole liable persons responsible for the authorship of this work, and that all material that has been herein included as part of the present paper is either the property (and authorship) of the authors, or has the permission of the owners to be included here.

## References

- [1] G.R. Liu and S.S. Quek. The finite element method. A practical course. Butterworth-Heinemann, 2003.
- [2] H.P. Wang, M.E. Botkin, C.T. Wu and S. He. Coupled finite element/meshfree simulation of manufacturing problems. *2003 ASME Pressure Vessels and Piping Conference*, pp. 1–6.
- [3] H. P. Wang, C.T. Wu, Y. Guo and M.E. Botkin. “A coupled meshfree/finite element method for automotive crashworthiness simulations”. *International Journal of Impact Engineering*, vol. 36, pp. 1210–1222, 2009.
- [4] G.R. Liu and Y.T. Gu. An introduction to meshfree methods and their programming. Springer, 2005.
- [5] E. Oñate. Structural analysis with the finite element method. Linear statics. Vol. 1. Basis and solids. Springer, 2009.
- [6] Altair HyperWorks. Desktop user guides. OptiStruct: Help. Version 2017.3.0, 2017. Electronic document available in Hypermesh-OptiStruct environment.
- [7] O.C. Zienkiewicz, R.L. Taylor and J.Z. Zhu. The finite element method. Its basis and fundamentals. Butterworth-Heinemann, 2005.
- [8] H. L. Soriano. Método de elementos finitos em análise de estruturas. Edusp, 2003.
- [9] G.R. Liu. Meshfree methods: Moving beyond the finite element method. CRC Press, 2010.
- [10] SimSolid 2020 Verification Manual. Available in: <<https://connect.altair.com/>>. Accessed on August 5<sup>th</sup>, 2020.